arXiv:1201.0468v2 [cond-mat.quant-gas] 21 Mar 2012

Boson and fermion dynamics in quasi-one-dimensional flat band lattices

M. Hyrkäs, V. Apaja and M. Manninen

Nanoscience Center, Department of Physics, FIN-40014 University of Jyväskylä, Finland

E-mail: vesa.apaja@jyu.fi

Abstract.

The difference between boson and fermion dynamics in quasi-one-dimensional lattices is studied with exact simulations of particle motion and by calculating the persistent current in small quantum rings. We consider three different lattices which in the tight binding model exhibit flat bands. The physical realization is considered to be an optical lattice with bosonic or fermionic atoms. The atoms are assumed to interact with a repulsive short range interaction. The different statistics of bosons and fermions causes different dynamics. Spinless fermions are easily trapped in the flat band states due to the Pauli exclusion principle, which prevents them from interacting, while boson are able to push each other out from the flat band states.

1. Introduction

Crystal structures existing in nature exhibit fascinating band structures which determine electronic, optical, magnetic and thermal properties of materials. The curvature of an energy band determines the effective mass of the electron which can be hundreds of times the normal mass, like in heavy fermion materials[1], or infinite, like in the kagome lattice[2] and other flat band lattices[3, 4], or even zero like in graphene[5].

Quantum dot lattices for electrons[6, 7, 8] and optical lattices for atoms[9, 10, 11, 12] have provided a new experimental setup where the lattice structure can be formed artificially and, consequently, also structures which do not exist in nature can be experimentally studied and utilized. Moreover, in optical lattices atom dynamics can be studied without problems caused by lattice defects or phonons[9, 13, 14] and the atoms trapped in the lattice can be chosen to be fermions or bosons.

The manipulation of the parameters of the optical lattice and the properties of the atoms allows variation of the size and even the sign of the hopping parameters between neighboring lattice sites.

In this paper we will study quasi-one-dimensional (Q1D) lattices with flat bands. Our motivation is the fast development in the research of atoms trapped in optical lattices, which has shown that surprisingly complicated lattice structures can be manufactured, such as the kagome lattice[15]. Recently we suggested how a flat band, 2D edge–centered square lattice could be made [16]. Such systems can be quite accurately described with a Hubbard Hamiltonian with contact interaction between the atoms. In the limit of an infinitely strong interaction only one atom can occupy each lattice site and consequently bosonic atoms will also have an "exclusion principle" in the simple (localized) tight binding basis of single particle states. However, bosons and fermions are different due to the different symmetry of the many-particle wave function. In this case of spinless particles the fermion wave function is a single Slater determinant, while the boson wave function is much more complicated consisting of many permanents. This causes interesting differences in the quantum dynamics of these two systems. For example, the time evolution of out–of–equilibrium bosons in 1D can be nonergodic[17]. The situation here is very different from that of a rotating two-dimensional harmonic trap where the vortex formation mechanisms in boson and fermion systems are closely related[18]. Trapped bosonic gas can be brought all the way to the infinite repulsion limit (Tonks–Girardeau gas), where bosons behave locally like free fermions - described as fermionization - but their momentum distribution is not fermionic[19]. Flat bands add a very intriquing flavor to the dynamics, as atoms occupying such band are essentially immobile, and allows us to contrast bosons and fermions.

In Section 2 we introduce three different Q1D lattices with flat bands. The simplest is a triangle lattice which has on flat band separated from a normal band. In the diamond lattice the flat band either cuts through two normal bands or can be separated from them. In the stub lattice a flat band and two normal bands are separated by energy gaps.

In Section 3 we introduce the many-body problem and describe how the dynamical simulations were made and the persistent currents calculated. In section 4 we describe the results for the persistent currents and in Section 5 the results for the dynamical simulations. The conclusions are given in Section 6.

2. Quasi-one-dimensional flat band lattices

There exists a large number of different lattice structures, which in the simple tight-binding model, with only one state per lattice site and only the nearest neighbor hopping, exhibit band structures with one or more flat bands[3, 4, 16]. Often the reason for the flat band is a solution where the single particle wave function is zero at some connecting sites of the lattice making it impossible for the particles to move through the lattice. These kind of lattices can be one, two or three dimensional.

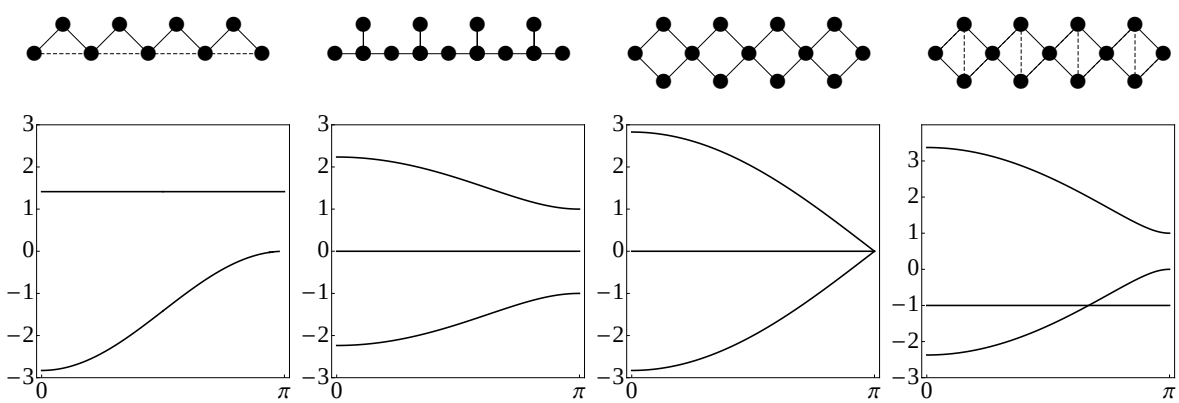

Figure 1. Band structures of the Q1D lattices studied: Triangle lattice, stub lattice, diamond lattice and diamond lattice with transverse hopping. The transverse axis shows the energy in units of $t = 1$ and the horizontal axis the k-value in units of the lattice constant. In the Triangular lattice the hopping parameter shown as a dashed line has the value $t' = 1/\sqrt{2}$. The parameter for the transverse hopping (dashed line) in the diamond lattice is $t' = -1$.

Figure 1 shows the Q1D lattices and the corresponding band structures studied in this paper. The single particle Hamiltonian is the Hückel-type tight-binding model

$$H_{\mathrm{TB}} = -\sum_{i,j}^{\mathrm{nn}} t_{ij} a_i^\dagger a_j, \tag{1}$$

where $a_i^\dagger$ creates a particle in lattice site i, t is the hopping parameter and 'nn' means that the sum is taken only over nearest neighbor sites. Throughout this paper we use natural units of the Hückel (or Hubbard) model where $t = 1$, $m = 1$, $\hbar = 1$.

In the triangle lattice the ratio of the two hopping parameters has to be $t/t' = \sqrt{2}$ in order to make one of the bands flat. For a positive t the flat band is above the normal band while for a negative t it is below. In the stub lattice the hopping parameter is the same between all neighbors. This lattice has a flat band in between the two normal

bands and separated from those by gaps. The diamond lattice also has three bands with the flat band in the center but in this case all the bands meet at the Brillouin zone boundary. Adding a transverse hop between two points in each diamond, as shown as a dashed line in the rightmost panel of Fig. 1, moves the flat band in relation to the other two bands. At the same time a gap opens between the two normal bands. Depending on the value of the transverse hopping parameter t', the flat band can cross a normal band (as show in the figure), or it can be below or above both of the normal bands.

In the cases of the stub lattice and the diamond lattice the reason for the flat band is that the wave functions of the flat band states are zero at the contact points of the unit cells, preventing any motion of particles from one unit cell to another. In the triangular lattice the reason for the flat band is more subtle as will be seen below when the persistent currents are considered.

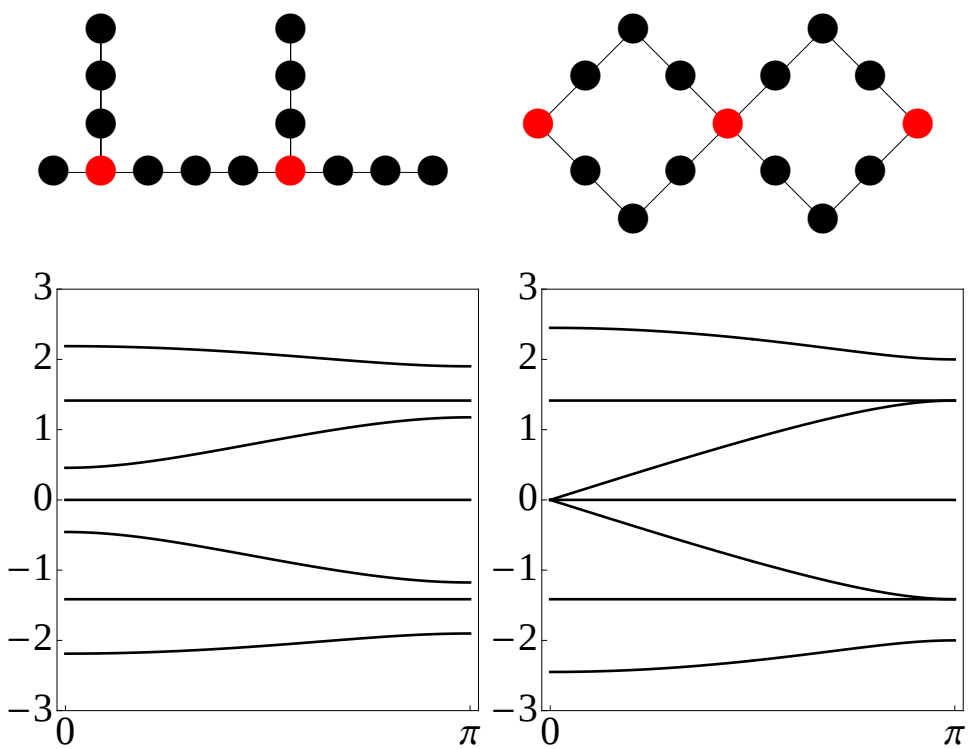

Figure 2. Band structures of extensions of the stub and the diamond lattices. The vertical axis shows the energy in units of $t = 1$ and the horizontal axis the k-value in units of the lattice constant. The red dots show the lattice sites at which the wave functions of the flat band states are zero.

The stub band and the diamond bands can be generalized to Q1D lattices with several flat bands as demonstrated in Fig. 2. In each flat band the wave functions are zero at the corner points shown as red dots. The positions of the flat bands are then determined by the length of the one-dimensional lattice (black dots) between the corner points. In both cases of Fig. 2 there are three sites between the corner sites. These sites can be thought to form a molecule with three sites and energy levels $(-\sqrt{2}, \quad 0, \quad \sqrt{2})$

in the tight binding model. These energy levels determine the positions of the flat bands which are then naturally same in both lattices.

3. Many-body dynamics

We consider atoms in an optical lattice and assume that the interaction between them has such a short range that it is only effective when the atoms are located in the same lattice site. We assume the atoms to be spinless or to be in the same spin state. In the case of fermionic atoms this means that the system is spin-polarized and thus each atom has the same z-component of spin. The many-body Hamiltonian describing the system is the Hubbard Hamiltonian

$$H = -\sum_{i,j}^{\mathrm{nn}} t_{ij} a_i^\dagger a_j + \sum_i V_i \hat{n}_i + \frac{U}{2} \sum_i \hat{n}_i(\hat{n}_i - 1), \tag{2}$$

where $\hat{n}_i = a_i^\dagger a_i$, V_i is a local potential and U is the strength of the contact interaction.

In the case of the spinless fermions the interaction term is irrelevant since the Pauli exclusion principle requires that each occupation n_i is either zero or one, and the many-body problem reduces to a single particle problem. The many-body state is a Slater determinant made out of the single particle wave functions which are solutions of the tight binding model.

In the case of bosons the situation is more complicated. If the repulsive interaction is infinitely strong we can assume that the occupation of each site can not be more than one. Unfortunately, this does not completely remove the complexity of the many-body problem like in the case of fermions. However, we can still neglect the interaction term of the Hamiltonian by restricting the Fock space to those states which have an occupation of 0 or 1 in each lattice site.

In solving the many-particle Hamiltonian in the case of bosons we use the localized basis in a finite length of the lattice and with a small number of particles. This restriction of the the computation to small systems has the advantage of allowing an exact diagonalization of the Hamiltonian. Alternatively, we can use the basis of matrix product states (MPS), where increasing the matrix dimensions increases the overlap with the exact state. Large systems, where exact diagonalization is impractical, can still be approximated by MPS with reduced matrix dimensions. Both the ground state representation as MPS and the time evolution of the state can be described using the time-evolving block decimation (TEBD) method by Vidal[20]. In TEBD one chooses a target size of the matrices, and as time evolution increases entanglement and thus expands the matrices, one truncates the matrices back to target dimensions by throwing out the least important contributions. What is important is determined by the means of repeated singular value or Schmidt decompositions. At least for a short time the truncation error does not affect results appreciably. TEBD propagates time step by step, leaving also a controllable time-step error to the results. In small systems both of these methods produced the same results.

We are interested in the effect of the flat bands on the many-body dynamics. To this end it is useful to know how the single particle states are occupied in a given many-body state. In the case of fermions this is trivial since the many-body state is a single determinant of the single particle states. In the case of bosons we can determine the occupations by changing the basis from the localized basis (α), where the many-body solution is $|\Psi\rangle = \sum_\alpha A_\alpha |\alpha\rangle$, to the TB basis ($\beta$), where $|\Psi\rangle = \sum_\beta B_\beta |\beta\rangle$. ($|\alpha\rangle$ and $|\beta\rangle$ are Slater determinants or permanents made of the single particle states). The occupations can be found without resolving the coefficients B_β by writing the annihilation operator of the TB basis as $b_j = \sum C_{ji} a_i$, where the coefficients C_{ji} are obtained from the TB solution. The occupation of a TB basis state k is then

$$n_k = \langle \Psi | b_k^\dagger b_k | \Psi \rangle = \sum_{\alpha,\alpha'} \sum_{i,j} A_\alpha^* A'_\alpha C_{ki}^* C_{kj} \langle \alpha | a_i^\dagger a_j | \alpha' \rangle. \tag{3}$$

The time dependence of the many-body state after a sudden change of the Hamiltonian (in our case the local potential) can be determined by solving the ground state of the many-body problem (for the initial potential) and all the many-body states for the final potential and expanding the initial state as

$$|\Psi\rangle = \sum_p D_p |\Psi_p\rangle, \tag{4}$$

where $|\Psi_p\rangle$ is the p'th time-independent energy state of the final Hamiltonian. The time-dependence now follows from the time-dependencies of the final states which are known:

$$|\Psi(t)\rangle = \sum_p D_p e^{-iE_p t} |\Psi_p\rangle, \tag{5}$$

where E_p is the energy eigenvalue of the state p. Note that in the case of fermions each final state is a Slater determinant. It then follows that the time dependence of the many-body state can be determined by following the time dependencies of the individual single-particle states. In principle, an initial local potential is actually not required, since one does not need to know the initial Hamiltonian, but only the initial state. One may, for example, prepare particles in certain lattice sites by any means conceivable, and then suddenly release them to follow the time evolution of the final Hamiltonian.

4. Persistent currents

Persistent currents in quantum rings with a few fermions have been extensively studied, for a review see[21]. In the case of bosons the early work was related to the research of macroscopic systems of ^{4}He[22, 23], while lately several studies of persistent currents in toroidal traps of bosonic atoms have been reported[24, 25, 26, 27, 28, 29].

There are several ways to produce a toroidal trap for atom condensates[24, 30, 31, 32, 33]. In the case of finite quantum rings made of the Q1D lattices considered, we induce an effective magnetic flux through the ring in order to induce a current. Neutral atoms do not interact with the magnetic flux in the same way as electrons in metallic or semiconducting quantum rings. Nevertheless, laser fields can generate phase change

which has the same effect as a magnetic flux[34, 35, 36]: An effective flux can be created using rotationally symmetric Laguerre-Gaussian laser modes.

In the Hubbard model a flux piercing the ring will cause a phase shift to the hopping parameter t_{ij} changing it to $e^{i\Phi_{ij}}t_{ij}$. In the case of the triangle lattice we have to notice that the phase shift Φ_{ij} is twice as large for the hop along the long edge of the triangle than along the short edges, i.e. the total phase shift is independent of the path of the particle from one point to another. In the case of the stub lattice the phase shift along stub is zero.

The persistent current can be determined as the derivative of the total energy as a function of the flux or computing the expectation value of the current operator between two points:

$$J = \frac{\partial E}{\partial \Phi} \quad \text{or} \quad J = i\sum_{i,j}^{\text{nn}} t_{ij} e^{i\Phi_{ij}} a_i^\dagger a_j. \tag{6}$$

In the case of bosons with infinitely strong contact interaction ($U \to \infty$) and no on-site potentials ($V_i = 0$) the Hamiltonian is the same for particles and holes, i.e. $H = \sum a_i^\dagger a_j = \sum a_j a_i^\dagger$ since the operators commute when $i \neq j$. This means that the ground state energy and the persistent current are symmetric with respect particles and holes, irrespective of the symmetry of the single particle spectrum. The situation is different for fermions due to the anticommutation rule, which changes the sign of the Hamiltonian for holes. Consequently, in the case of fermions the many-body energy and the persistent current are symmetric with respect to particles and holes only if the single particle spectrum is symmetric.

We will study the persistent current in the flat band lattices with exact diagonalization of the Hubbard Hamiltonian in small systems. For bosons we assume an infinitely strong contact interaction and for fermions we assume the system to be spin-polarized. In the strictly one-dimensional case both boson and fermion systems are exactly solvable via the Bethe ansatz[37, 38, 39, 40]. However, already in the strictly 1D case the bosons and the fermions differ due to the different symmetry of the wave function. In both cases the current is a periodic function of the flux through the ring, but depending on the number of the particles the periodicity can have a different phase for fermions and bosons. In the case of a zero flux, the lowest energy state for any number of bosons has a zero angular momentum while for an odd number of spinless fermions the lowest energy state has a finite angular momentum ($L = N/2$)[21, 29], resulting in a finite current with an infinitesimal flux.

In the strictly one-dimensional case spinless fermions can not pass each other. The same is true for bosons interacting with an infinitely strong delta function interaction. The flat band lattices are necessarily quasi-one-dimensional and thus more complicated.

We studied the persistent currents in flat band lattices by solving exactly the Hubbard model for rings with a small number of lattice sites. Figure 3 shows the results for rings made of the stub and and diamond lattices. In each case the ring has 12 sites and from 1 to 11 atoms (for 12 particles all the sites are occupied and no current

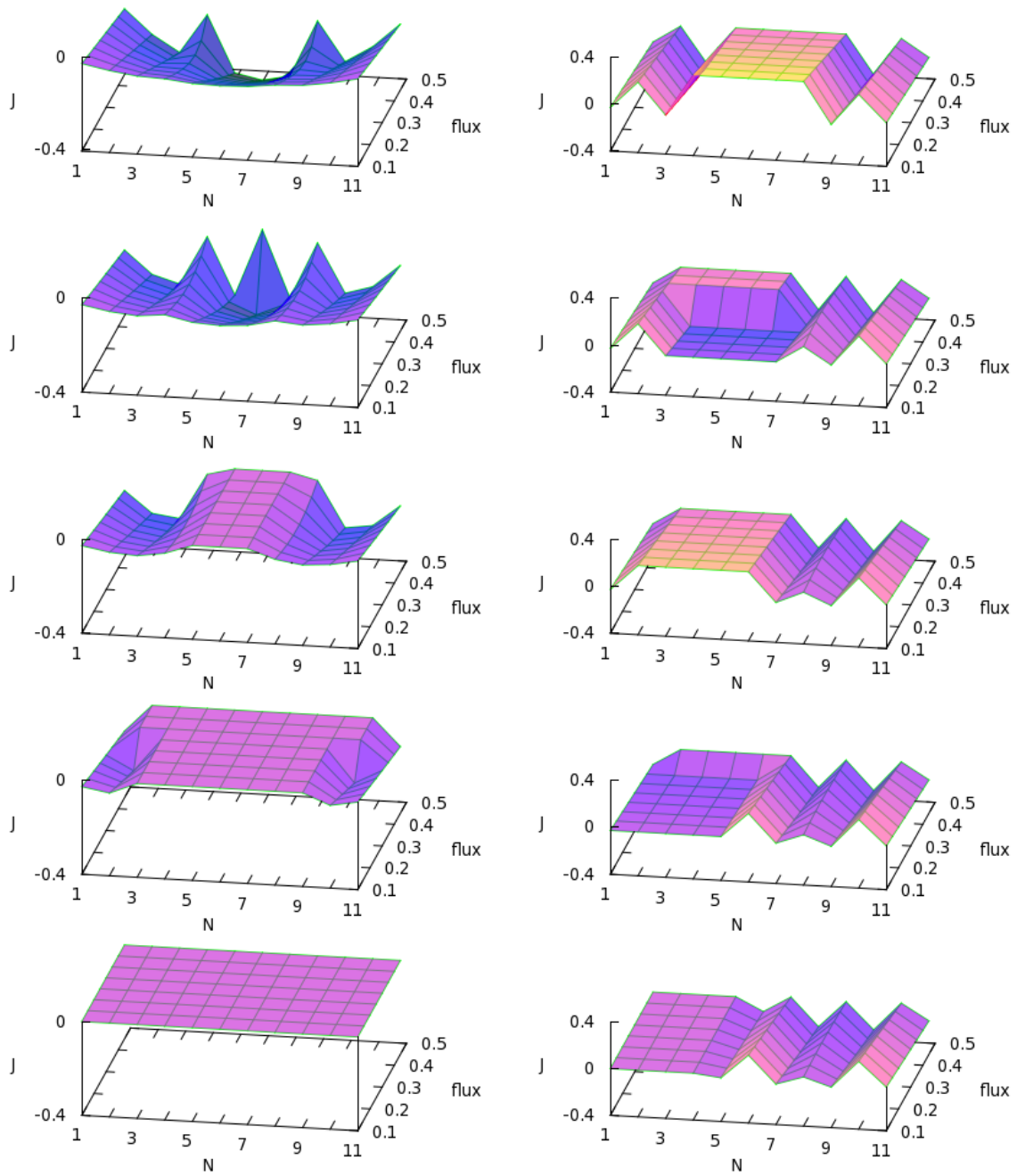

Figure 3. Persistent current of bosons (left) and fermions (right) in quantum rings made of four unit cells of the diamond lattice. The current J is shown as a function of the number of particles in the ring (N) and the flux. In the upmost figures the flat band is in between the normal bands, and finally, in the lowest figures, below the normal bands (controlled by the value of the transverse hopping parameter, using values $t' = 0, 1.0, 1.5, 1.8, 2.1$). As the flat band moves down in energy, bosons occupy it more and more, finally leaving all bosons immobile. As particles are added, fermion current changes sign, except that it remains constant during filling of the flat band. The stub lattice gives results similar to the upmost figures.

can flow). We notice that the bosonic and the fermionic cases are markedly different. When the flat band is symmetrically in the middle between the two normal bands (two uppermost cases in the figure), the current shows a particle-hole symmetry, i.e. the result is the same for N atoms and for $12 - N$ atoms.

In the case of bosons the current as a function of the flux for 4 and 8 atoms is qualitatively different from that for other atom numbers. In the case of fermions the current is independent of the particle number when the flat band is filled. This is because the system is noninteracting and the flat band can not conduct. The $N = 2$ case has a finite current already at zero flux. This is because in the single particle picture this state has an angular momentum of 1 (or -1) and thus a current. In the case of the stub lattice the current for four particles and small flux is zero because the lowest band is full. In the case of the diamond lattice both normal bands meet the flat band at the Brillouin zone boundary. Due to this degeneracy we get a finite current for an infinitely small flux for particle numbers $N = 4 \ldots 8$.

The lowest panel in Fig. 3 shows the results for the diamond lattice where the transverse hopping shown in Fig. 1 has a value $t' = -2.1$, which brings the flat band below both of the normal bands. In this case the persistent current for bosons is always zero. For fermions it is zero only for particle numbers $N = 1 \cdots 4$, which fit in the flat band. For particle numbers 6 and 10 the ground state is degenerate and the current start from a finite value.

The results for the triangle lattice are shown in Fig. 4. The top panel shows the results for the case where the flat band is on top of the normal band (positive t'), while in the lower panel the flat band is below the normal band (negative t'). Note that the band structure does not depend on the sign of t.

In both cases the current for bosons has a particle-hole symmetry, i.e. the current is the same for N and $12 - N$ particles, as discussed in the previous section. This symmetry causes a surprising effect when the flat band is at the bottom: The boson current is zero for all flux values not only for small particle numbers ($N = 1$, 2 and 3) but also for large particle numbers ($N = 9$, 10 and 11).

The triangle lattice has the interesting feature that even when the total persistent current is zero there is a current going around in each triangle. This is demonstrated in the case of two particle in Fig. 5, which shows separately the currents going along the short edge of the triangle and along the long edge. When the flat band is at the bottom, the total current is zero, but the currents going along the short and long edges are nonzero with opposite signs. This means that the flux, which is zero inside the triangles, still induces a current going around each triangle.

In the case where the flat band is at the top, the currents along the short and long edges of the triangles go to the same direction, but have different magnitudes. Figure 5 also demonstrates that the currents are periodic functions of the flux. In the fermionic case there is a discontinuity at integer flux values and in the case of bosons at half-integer flux values. These discontinuities are caused by the degeneracies of the many-body state.

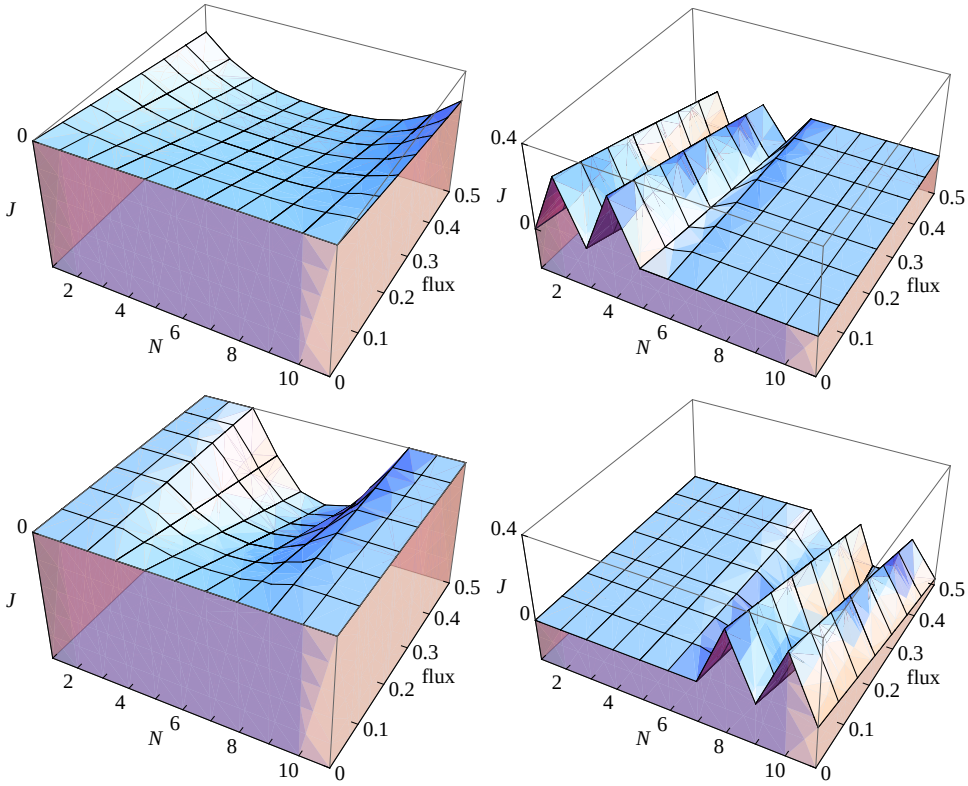

Figure 4. Persistent current of bosons (left) and fermions (right) in quantum rings made of six unit cells of the triangle lattice. The current (vertical coordinate) is shown as a function of the number of particles in the ring (N) and the flux. Note the different scale of the current for bosons and fermions. In the upper panel the flat band is above the normal bands (t' positive) and in the lower panel the flat band is below the normal bands (t' negative).

5. Simulations of particle motion

The results of the previous section show that for some particle numbers the current through the ring is zero independently of the value of the flux. This suggests that the particles can be localized at the flat band states. In order to study the localization further we performed simulations of the dynamics. Initially the particles were confined to a certain region of the lattice by adding a harmonic confinement $V_{\mathrm{h}}(i) = \alpha i^2$, where i is the distance from the bottom of the harmonic confinement (in units of the distance between the lattice sites along the ring) and α is the strength of the potential. Since we are interested only in qualitative differences we chose $\alpha = 1$.

We studied the dynamics of four particles in a diamond lattice with 21 sites and in a triangle lattice with 22 sites. In each case we solved the lowest energy state of the Hubbard Hamiltonian with the harmonic confinement and fully diagonalized the Hamiltonian for the final state, i.e. without the harmonic potential. This allowed us (using Eq. (5)) to study how the particles move when the harmonic confinement is suddenly removed.

Figure 6 shows the results for the diamond lattice with 21 sites and periodic

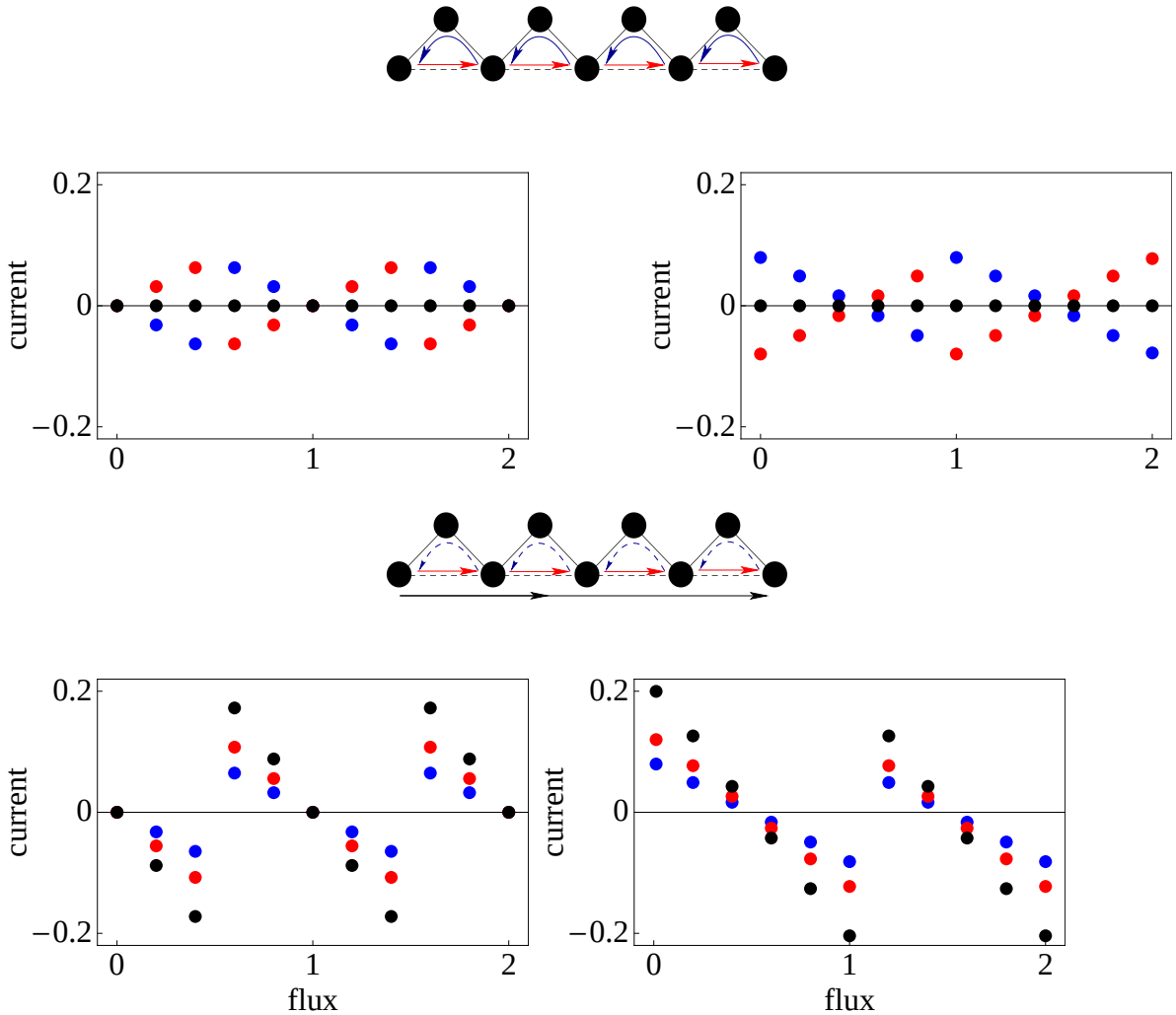

Figure 5. Current components of two fermions and bosons in a quantum ring of the triangular lattice. The black dots show the total current and the red and blue dots the currents along the long edge and the short edge of the triangle, respectively. The left panels show the results for bosons and the right panels for fermions. The upper panels are for the case where the flat band is below the normal band, resulting in zero net current. The lower panels are for the case where the flat band is above the normal band.

boundary conditions. The lattice sites were numbered in succession so that the contact sites are 1, 4, 7, 10, etc. and the two other sites in each diamond 2, 3, 5, 6, 8, 9, 11, 12, etc. The center of the harmonic confinement was set at the sites 11 and 12, so that the potential was $V_{11} = V_{12} = 0$, $V_{10} = V_{13} = 1$, $V_9 = V_8 = V_{14} = V_{15} = 4$, and so on. Initially the particles are localized around the sites 11 and 12. When the potential is removed the particles start to move outwards until they reach the borders of the simulation cell and start to overlap with the particles arriving from the neighboring cells (due to the periodic boundary conditions).

The upper panel shows the results for the case where the flat band is in between

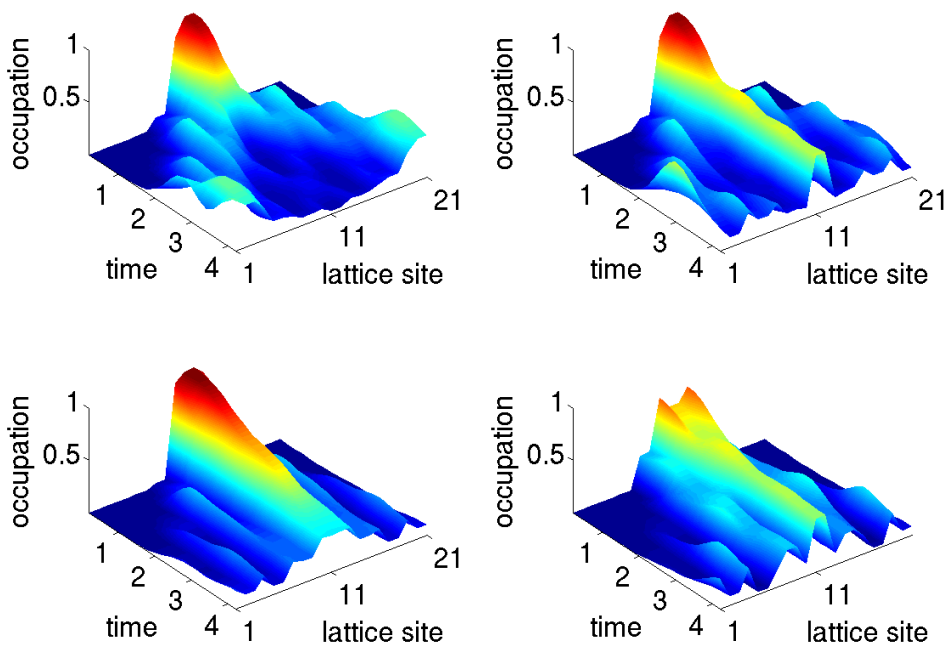

Figure 6. Particle density (occupation) at different lattice sites of the diamond lattice as a function of time after the harmonic confinement is removed. The left panels show the results for bosons and the right panels for fermions. The upper figures show the results for the case where the flat band is in between the normal bands ($t' = 0$) and the lower figures for the case where the flat band is below the normal bands ($t' = -2.1$).

the normal bands. In this case all the bosons become mobile and fly away, while some of the fermions stay at the sites 11 and 12. The situation is not changed much when the flat band is below the normal bands. Also in this case the bosons fly away but now more slowly. the initial fermion distribution is wider but again some of the fermions stay immobile. We also computed the dynamics for the stub lattice with 21 sites. The results were qualitatively similar to those of the diamond lattice with the flat band at the center.

Figure 7 shows the results for the triangle lattice. In this case we have 22 lattice sites and the center of the harmonic confinement is at the site 11. The initial potentials are $V_{11} = 0$, $V_{10} = V_{12} = 1$, $V_9 + V_{13} = 4$, $V_8 = V_{14} = 9$ and so on. The upper panel of Fig. 7 shows the cases where the flat band is at the top and the lower panels the cases where the flat band is at the bottom. The results are rather similar to those for the diamond lattice. In both cases the boson distribution widens with time and all the bosons eventually fly away. Also in both cases a part of the fermions stays localized.

We have repeated the dynamics simulations for different particle numbers and numbers of lattice sites, using both periodic boundary conditions and a finite length lattice. In all cases the results are qualitatively similar to those shown in Figs. 6 and 7.

The general result, that some of the fermions stay localized in the flat band states, is easy to understand. Spinless fermions with contact interaction are equivalent to

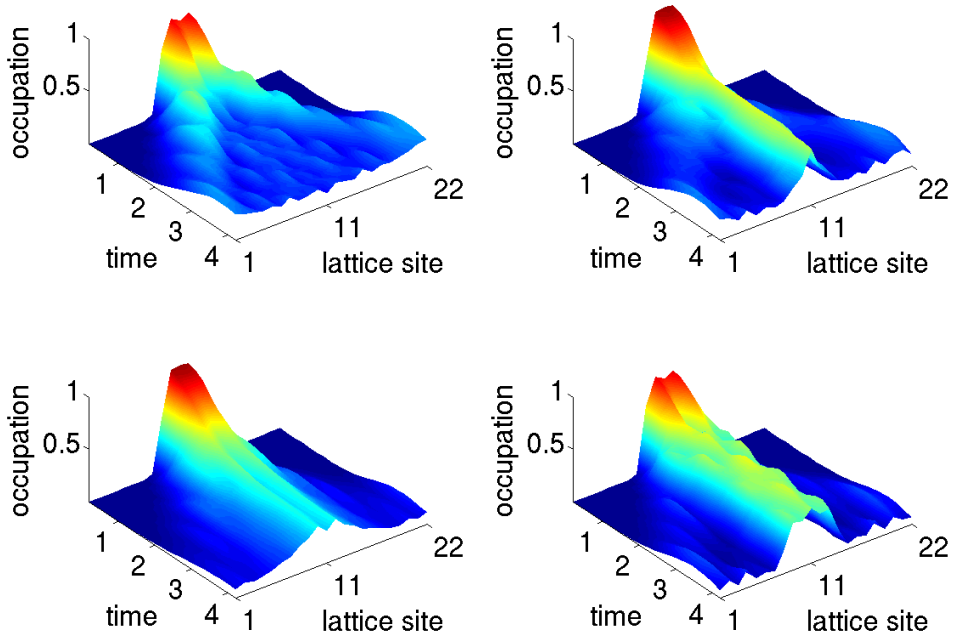

Figure 7. Particle density (occupation) at different lattice sites of the triangle lattice as a function of time after the harmonic confinement is removed. The left panels show the results for bosons and the right panels for fermions. The upper figures show the results for the case where the flat band is above the normal band (t' positive) and the lower figures for the case where the flat band is below the normal band (t' negative).

noninteracting fermions. Those initially occupying a flat band state will stay there when the confinement potential is removed. The same is not true for bosons, which can push each other out from the flat band states.

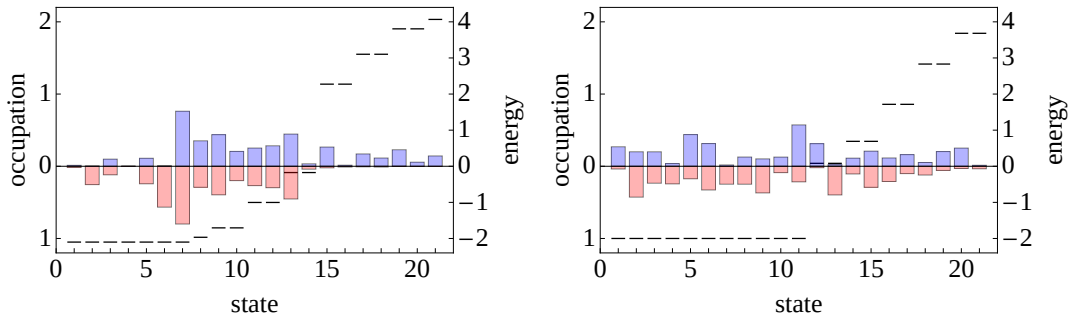

Figure 8. Occupation of single particle levels in the initial many-body state (in the presence of the harmonic confinement). The single particle energy levels (without the confinement) are shown as short lines and the corresponding occupancies as bars, blue for bosons and red for fermions. Left: Diamond lattice with the flat band at the bottom. Right: Triangle lattice with the flat band at the bottom.

In the cases where the flat band is the lowest band the initial boson and fermion

distributions are slightly different. In order to get more insight to the initial many-body state we determined the single particle occupancies using Eq. (3) for bosons and fermions. The results are shown in Fig. 8. The figure shows that the many-body state of the bose systems has nearly as large occupancy of the flat band states as the fermi system. In fermion systems those particles are immobile, but in boson systems they interact with the particles in the normal band, and become mobile.

6. Conclusions

We have addressed the differences in particle dynamics between bosons and fermions in quasi-one-dimensional lattices with a flat band. The particles were assumed to be spinless and interacting with an infinitely strong contact interaction. In this case the fermions are equivalent to noninteracting particles due to the Pauli exclusion principle. Consequently, the fermions occupying the flat band states do not contribute to the persistent current in a quantum ring, and they are localized in the lattice.

In the case of bosons the particles are truly interacting making the system more interesting. The persistent current shows a particle-hole symmetry and the occupation of the flat band can also change the current. The bosons do not stay localized in the lattice even if initially the partition of the many-body wave function to the single particle states is essentially the same as in the case of fermions.

These results are very general, they do not seem to depend on the detailed structure of the lattice or on the position of the flat band with respect to the normal bands with dispersion.

Acknowledgments: Ideas for this work were initiated by a workshop of the European Science Foundation research networking program POLATOM. We thank the Academy of Finland for financial support.

[1] G R Stewart. *Rev. Mod. Phys.*, 56:755, 1984.
[2] I Syoẑi. *Prog. Theor. Phys.*, 6:306, 1951.
[3] S Deng, A Simon, and J Köhler. *J. Solid State Chem.*, 176:412, 2003.
[4] S Miyahara, K Kubo, H Ono, Y Shimomura, and N Furukawa. *J. Phys. Soc. Japan*, 74:1918, 2005.
[5] A H Castro Neto, F Guinea, N M R Peres, K.S. Novoselov, and A.K. Geim. *Rev. Mod. Phys.*, 81:109, 2009.
[6] H Lee, J A Johnson, M Y He, J S Speck, and P M Petroff. *Appl. Phys. Lett.*, 78:105, 2001.
[7] M Koskinen, S M Reimann, and M Manninen. *Phys. Rev. Lett.*, 90:066802, 2003.
[8] S M Reimann and M Manninen. *Rev. Mod. Phys*, 74:1283, 2002.
[9] I Bloch. *Nature Physics*, 1:23, 2005.
[10] A J Legget. *Quantum Liquids: Bose condensation and Cooper pairing in condensed matter physics.* Oxford University Press, 2006.
[11] C J Pethick and H Smith. *Bose-Einstein Condensation in Dilute Gases.* Cambridge University Press, 2 edition, 2008.
[12] S López-Aguayo, Y V Kartashov, V A Vysloukh, and L Torner. *Phys. Rev. Lett.*, 105:013902, 2010.
[13] I Bloch. *Science*, 319:1202, 2008.
[14] I Bloch, J Dalibard, and W Zwerger. *Rev. Mod. Phys.*, 80:885–964, 2008.

[15] Gyu-Boong Jo, Jennie Guzman, Claire K. Thomas, Pavan Hosur, Ashvin Vishwanath, and Dan M. Stamper-Kurn. Ultracold atoms in a tunable optical kagome lattice. *Phys. Rev. Lett.*, 108:045305, Jan 2012.
[16] V Apaja, M Hyrkäs, and M Manninen. *Phys. Rev. A*, 82:041402, 2010.
[17] Toshiya Kinoshita, Trevor Wenger, and David S. Weiss. A quantum newton's cradle. *Nature*, 440(7086):900–903, Apr 2006.
[18] H Saarikoski, S M Reimann, A Harju, and M Manninen. *Rev. Mod. Phys.*, 82:2785, 2010.
[19] Belen Paredes, Artur Widera, Valentin Murg, Olaf Mandel, Simon Folling, Ignacio Cirac, Gora V. Shlyapnikov, Theodor W. Hansch, and Immanuel Bloch. Tonks-girardeau gas of ultracold atoms in an optical lattice. *Nature*, 429(6989):277–281, May 2004.
[20] G Vidal. *Phys. Rev. Lett.*, 93:040502, 2004.
[21] S Viefers, P Koskinen, P Singha Deo, and M Manninen. *Physica E*, 21:1, 2004.
[22] J D Reppy and D Depatie. *Phys. Rev. Lett.*, 12:187, 1964.
[23] W Grobman and M Luban. *Phys. Rev.*, 147:166, 1966.
[24] Y Lyanda-Geller and P M Goldbart. *Phys. Rev. A*, 61:043609, 2000.
[25] T Isoshima, M Nakahara, T Ohmi, and K Machida. *Phys. Rev. A*, 61:063610, 2000.
[26] T Wang, J Javanainen, and S F Yelin. *Phys: Rev. A*, 76:011601, 2007.
[27] C Ryu, M F Andersen, P Cladé, V Natarajan, K Helmerson, and W D Phillips. *Phys Rev Lett*, 99:260401, 2007.
[28] S Bargi, F Malet, G M Kavoulakis, and S M Reimann. *Phys. Rev. A*, 82:043631, 2010.
[29] V E Lembessis and M Babiker. *Phys. Rev. A*, 82:051402, 2010.
[30] A Hopkins, B Lev, and H Mabuchi. *Phys. Rev. A*, 70:053616, 2004.
[31] O Morizot, Y Colombe, V Lorent, H Perrin, and B M Garraway. *Phys. Rev. A*, 74:023617, 2006.
[32] P F Griffin, E Riis, and A S Arnold. *Phys. Rev. A*, 77:051402, 2008.
[33] P M Baker, J A Stickney, M B Squires, J A Scoville, E J Carlson, W R Buchwald, and S M Miller. *Phys. Rev. A*, 80:063615, 2009.
[34] E J Mueller. *Phys. Rev. A*, 70:041603, 2004.
[35] L Amico, A Osterloh, and F Cataliotti. *Phys. Rev. Lett.*, 95:063201, 2005.
[36] A L Fetter. *Rev. Mod. Phys.*, 81:647, 2009.
[37] E H Lieb and W Liniger. *Phys Rev*, 130:1605, 1963.
[38] E H Lieb. *Phys Rev*, 130:1616, 1963.
[39] C N Yang. *Phys Rev Lett*, 19:1312, 1967.
[40] E H Lieb and F Y Wu. *Phys. Rev. Lett.*, 20:1445, 1968.